Energy Conversion and Management xxx (xxxx) 118642

Contents lists available at ScienceDirect

Energy Conversion and Management

journal homepage: www.elsevier.com/locate/enconman

Valorisation of tyre waste from a vulcanisation plant by catalytic pyrolysis – Experimental investigations using pyrolysis–gas chromatography–mass spectrometry and drop-tube–fixed-bed reactor

Wojciech Jerzak, Mariusz Wądrzyk, Małgorzata Sieradzka, Aneta Magdziarz

AGH University of Krakow, Mickiewicza 30, 30-059 Krakow, Poland

ARTICLE INFO

Keywords:
End-of-life tyres
Pyrolysis
Drop-tube reactor
Catalyst
Tyre ash

ABSTRACT

This study focuses on the use of car tyre waste collected at a tyre repair station in Krakow (Poland). Waste from damaged tyres is disposed of as municipal solid waste. Therefore, the management of waste tyres already shredded by pyrolysis at 500 °C has been proposed. Tyre waste was hypothesised to be converted into valuable chemical products by pyrolysis in a hybrid reactor (drop-tube–fixed-bed reactor). On a micro scale, pyrolysis–gas chromatography–mass spectrometry was used to analyse the pyrolysis process. It has been shown that the formation of aromatic hydrocarbons during pyrolysis clearly depends on whether the catalyst and tyre waste are mixed together or arranged in layers. Since the layered arrangement favoured the formation of hydrocarbons, such a system was used in the drop-tube–fixed-bed reactor. The high heating rate (500 °C/s) of tyre particles in the drop-tube–fixed-bed reactor at 500 °C allowed for the obtained a raw carbon black yield of 40.8 %. A similar yield of raw carbon black determined by thermogravimetric analysis for a heating rate of 0.17 °C/s) was observed at 800 °C. However, before commercial use, raw carbon black requires demineralisation because of its high ash content (approximately 50 %). The raw carbon black ash contained up to 90 % SiO_2, indicating that it could be a valuable catalyst material.

Pyrolysis of tyre waste over the catalyst reduced the oxygen content in the oil and yield. The oil yields of tyre pyrolysis without a catalyst and over zeolite Y were 38 wt% and 35 wt%, respectively. The main components identified in the tyre pyrolysis gas were methane (27.6%), ethene (28.8%), and hydrogen (15.6%). The gas from catalytic pyrolysis was richer in CO and CO_2.

Nomenclature

Abbreviations

A	Ash
AR	Auger reactor
cat	Catalyst
CFLBR	Circulating fluidised-bed reactor
CSBR	Conical spouted-bed reactor
DTG	Derivative thermogravimetry
DTR	Drop-tube reactor
DT-FBR	Drop-tube–fixed-bed reactor
ELTs	End-of-life tyres
FBR	Fixed-bed reactor
FC	Fixed carbon
FLBR	Fluidised-bed reactor
FT-IR	Fourier-transform infrared
FR	Feed rate
HHV	Higher heating value
HR	Heating rate
HTO	High-temperature oxidation
LTO	Low-temperature oxidation
M	Moisture
MTO	Mid-temperature oxidation
PS	Particle size
Py-GC–MS	Pyrolysis–gas chromatography–mass spectrometry
rCB	Recovered carbon black
RKR	Rotary kiln reactor
S/C	Sample-to-catalyst ratio
T	Pyrolysis temperature

E-mail address: wjerzak@agh.edu.pl (W. Jerzak).

https://doi.org/10.1016/j.enconman.2024.118642
0196-8904/© 20XX

TGA	Thermogravimetric analysis
TIC	Total ion chromatograms
TPG	Tyre pyrolysis gas
TPO	Tyre pyrolysis oil
TW	Tyre waste
VM	Volatile matter
VRT	Vapour residence time
XRF	X-ray fluorescence

1. Introduction

Producing fuels and chemicals from waste and biomass is an appropriate way to decrease the carbon footprint associated with the use of fossil fuels in energy production. End-of-life tyres (ELTs) are a noteworthy waste that can be used to obtain recovered carbon black (rCB), tyre pyrolysis oil (TPO), tyre pyrolysis gas (TPG), and steel from pyrolysis. The carbon footprint of producing TPO, rCB, and steel in this manner is 80 % smaller than that of conventional production based on fossil fuels [1]. In Poland, according to data from 2019, 268.5 thousand tons of new tyres were produced, of which the total material and energy recoveries were 47.3 % and 31.3 %, respectively [2]. ELTs are calorific wastes whose higher heating value (HHV) ranges from 33.4 to 38.6 MJ/kg [3]. ELTs consist of 14–48 wt% natural rubber, 10–27 wt% synthetic rubber, 11–28 wt% carbon black, 14–25 wt% steels, and 12–17 wt% fabric, fillers, accelerators, and antiozonants [4]. Truck tyres contain more steel and natural rubber than car tyres [5].

Although research on the pyrolysis of ELTs has been conducted for more than 50 years [6], the quality, yield, and application of the pyrolysis products still require further improvement in many aspects. The thermal treatment of ELTs by pyrolysis is not always effective due to inadequate control of raw materials, material heterogeneity, or a too high pyrolysis temperature [7]. The quality and yield of the pyrolysis products of ELTs depend primarily on the operating conditions of the process, which are classified as flash, fast, intermediate, and slow [8]. The use of high heating rates of approximately 1000 °C/s and short vapour residence times (VRTs) in the reactor favour the production of TPO via the fast pyrolysis process. Three other factors that determine the quality and yield of the pyrolysis products are the types of reactor, catalyst used, and pressure [9]. The reactors used for the ELTs pyrolysis are summarised in Table 1. A fixed-bed reactor is commonly used for the pyrolysis of ELTs at the laboratory scale [10]. Regardless of the reactor type, i.e., (i) horizontal fixed-bed, (ii) vertical fixed-bed, or (iii) one/two-step catalytic bed, they operate only in the batch mode. ELTs pyrolysis over the zeolite-Y catalyst in a fixed-bed reactor produced significantly higher concentrations of benzene, toluene, xylenes, naphthalene, and alkylated naphthalene's compared to the ZSM-5 catalyst [11]. Boxiong et al. [12] suggested that, a catalyst/tyre ratio of 0.5 provides the best balance between maximizing the production of certain aromatic hydrocarbons and maintaining an acceptable overall oil yield. A comparison between microporous and mesoporous catalysts showed that microporous zeolite Y catalysts produced higher C8-C12 hydrocarbon production, reaching up to 27 % carbon [13]. At the same time, zeolite Y exhibited higher coke formation during the pyrolysis reaction compared to the MCM 41 catalyst. Fluidised-bed reactors and circulating fluidised-bed reactors are popular in industry, which is due not only to the high yield of TPO, but also to its ability to operate continuously [14]. The use of catalysts with different surface acidities and selective porosities (zeolite Y and ZSM-5) allowed to obtain similar concentrations of chemicals in the product oil [15]. This similarity was attributed to the short residence times of gases in the catalytic fluidised –bed reactor.

A conical spouted bed reactor (CSBR) can be considered as a simpler design for a fluidised bed reactor without a distribution plate. Both the design of the CSBR, which forces a short residence time for the ELTs particles, and the high intensity of heat and mass transfer between the solid and gaseous phases promote a high TPO yield [17]. Poor-quality rCB have been reported in conical spouted-bed reactors that need to be activated [18]. In the category of reactor mobility, that is, the ability to move the reactor to any place where ELTs are stored, the auger reactor is incomparable. The TPO yields at 500 °C were of good quality and equal to more than 40 % of the product yields [19]. In commercial and semi-commercial tyre pyrolysis systems, the TPO production yield ranges from 45 to 52 wt% [24]. Pyrolysis of ELTs with CaO addition effectively reduced the sulphur content and also led to a decrease in the viscosity of TPO, which improves its potential usability as a fuel [20]. The screw system must be constantly monitored to prevent feedstock buildup and reactor clogging. ELTs are typically ground into irregular shapes prior to pyrolysis. The variable shape and size of the feed material are not a problem in rotary kiln reactors [21]. However, such reactors are characterised by a nonuniform temperature distribution in the radial and axial directions. Consequently, the temperature stability of the pyrolysis process is low. The application of spent fluid-catalytic-cracking (FCC) catalysts in the pyrolysis of ELTs resulted in an increase in the pyrolysis oil yield [22]. The content of light aromatic compounds in the pyrolysis products increased by more than 90 % when utilizing spent FCC catalysts. Providing a uniform temperature along the length of the drop-tube reactor is challenging [23]. In general, the longer the reactor, the more difficult it is to ensure a uniform temperature.

The last parameter that determines the pyrolysis products is the pressure. Pressurized pyrolysis and subsequent processes such inline catalytic cracking and steam reforming can significantly increase the yield of desired products such as single-ring aromatics and methane [25].

This paper presents the results of experimental research on car tyre waste (TW) pyrolysis using a drop-tube–fixed-bed reactor (DT-FBR). The use of DT-FBR contributes to going beyond the state-of-the-art approaches. According to the literature review, no experimental studies of catalytic pyrolysis in this type of reactor have been conducted yet. It was hypothesized that utilizing DT-FBR, in the pyrolysis process of tyre waste will result in the formation of specific chemical products with higher yields and improved quality compared to other type of reactors. Moreover, compared to previously published studies on catalytic pyrolysis of tyres in fixed-bed reactors, a research gap was filled regarding the formation of pyrolysis products when the catalyst was or was not mixed with tyre waste.

The aim of this work was also to demonstrate the possibility of using TW that is currently landfilled. The results of these studies may encourage vulcanisation plants to collect and manage TW sustainably.

Table 1
ELTs pyrolysis reactors—analysis of the state-of-the-art.

Pyrolysis reactor	Non-catalytic pyrolysis	Catalytic pyrolysis
	Reference	
Fixed-bed reactor (FBR)	[10]	[11–13]
Fluidised-bed reactor (FLBR)	[14]	[15]
Circulating fluidised-bed reactor (CFLBR)	[16]	No research
Conical spouted-bed reactor (CSBR)	[17]	[18]
Auger reactor (AR)	[19]	[20]
Rotary kiln reactor (RKR)	[21]	[22]
Drop-tube reactor (DTR)	[23]	No research
Drop-tube–fixed-bed reactor (DT-FBR)	No research	No research

2. Materials and methods

ELTs in Poland can be utilised through combustion, gasification, or pyrolysis for the production of new materials and the recovery of chemical energy. In vulcanisation plants, in addition to ELT collection, car tyre waste (TW) is generated, which is not segregated and enters landfills. TW was selected as the raw material for pyrolysis to use of its energy potential and avoid landfilling.

2.1. End-of-life tyres and catalyst characterization

TW fraction of 500–5000 μm was collected at a car tyre repair station in Krakow (Poland). After sieving, this TW fraction does not need to be ground using energy; thus, it could be a favourable feedstock for thermal conversion. The inter-sieve fraction of 500–800 μm containing 6.45 % of steel was used for the investigations. Typically, ELTs analysed in the literature are pretreated to remove steel components [26]. The samples prepared for pyrolysis in this study contained steel and are abbreviated as TW. The TW fed into the pyrolysis process contained steel as there were some difficulties in the magnetic separation of the steel from the TW; however, the presence of iron could act as a catalyst. The proximate and ultimate analyses of TW are presented in Table 2. Ultimate analysis was performed using a Vario Micro Cube elemental analyser (Elementar, Germany). The literature values of proximate and ultimate analyses of ELTs range widely. Tyre tread rubber (TTR) has a different composition from that of sidewall rubber (SWR). SWR contains four times less ash than TTR (2.14 % and 18.04 %, respectively) [27]. Moreover, depending on the type of tyre (cars, trucks, and agricultural vehicles), tyres can contain 54.01–89.5 % carbon. Owing to the high carbon content of the ELTs, standards for coal were used for the proximate and ultimate analyses. TW was characterised by a high ash content (21.40 %), which promoted an increased yield of rCB during pyrolysis.

The tar formed during pyrolysis easily accumulates on the walls of the lines connecting the ice cooler to the rCB bin. They not only make it difficult to precisely determine the TPO yields, but also reduce the diameter of the lines. The use of a catalyst for pyrolysis minimises tar formation and improves the quality of the obtained TPO. In this study, a zeolite Y catalyst (Si/Al ratio of 26.3; specific surface area of 780 m^2/g) purchased from Alfa Aesar was used. The zeolite Y was first calcinated at 550 °C for 3 h to remove moisture and activate the catalyst before TW pyrolysis. A silica–aluminium acid catalyst such as zeolite Y is a good choice for improving both the selectivity of TW pyrolysis products and the cracking process.

Table 2
Proximate and ultimate analyses of studied TW and reference data for ELTs.

Proximate and ultimate analyses, wt.%, [a] *ad*			
Parameter	Standard	Present study	Reference
Moisture (M)	ISO 18134–2:2017–03	0.94 ± 0.08	0.4 [28] – 2.67 [29]
Volatile Matter (VM)	ISO 562:2010	65.14 ± 0.24	56.72 [4] – 83.9 [30]
Ash (A)	ISO 1170:2010	21.40 ± 0.10	2.14 [27] – 22.80 [31]
Fixed Carbon (FC [b])	ISO 1213–2:2016	12.52 ± 0.42	7.30 [30] – 36.90 [32]
C	ISO 29541:2010	68.31 ± 0.14	54.01 [31] – 89.50 [4]
H	ISO 29541:2010	6.76 ± 0.06	4.73 [31] – 8.2 [20]
N	ISO 29541:2010	0.31 ± 0.04	<0.1 [20] – 1.0 [4]
S	ISO 19579:2006	1.61 ± 0.10	0.29 [27] – 3.31 [5]
Cl	ISO 587:2000	0.05 ± 0.05	0.21 [31]– 0.39 [10]
O[c]	ISO 17247:2020	0.72 ± 0.34	0.40 [33] – 21.72 [29]

[a] *ad*: air dried basis.
[b] FC = 100 − M − VM − A.
[c] By difference O = 100-(C + H + N + S + A + M·16/18).

2.2. Methods

A Vario Micro Cube elemental analyser (Elementar, Germany) was also employed to rCB, TPO and catalysts ultimate analysis. A Fourier-transform infrared (FT-IR) spectrometer (Bruker Alpha II) was used to identify the functional groups and types of bonds in the TW, catalyst (raw and used), TPO, and rCB. The infrared absorption frequency ranged from 400–4000 cm^{-1}. Thermogravimetric analysis (TGA) was performed using a Mettler Toledo STA apparatus to investigate the TW pyrolysis. The process parameters were as follows: i) alumina crucible (Al_2O_3), ii) sample mass (5 mg), iii) nitrogen atmosphere (40 mL/min), iv) heating rate (10 °C/min), and v) temperature range (25–800 °C). The TPO obtained using the DT-FBR was also evaluated. The TPO oxidation process in air was also analysed using TGA. In the sapphire crucible, 5 mg of sample was loaded and heated from 25 up to 700 °C at 10 °C/min with an air flow rate of 40 mL/min. An Agilent Technology 7890 gas chromatograph (GC) was used to analyse the components of the pyrolysis gas. To analyse the composition of tyre oils, an Agilent 7890B GC was used in combination with mass spectrometry technique (model: 5977A). After rCB was ashed at a temperature of 815 °C, its composition and zeolite Y were analysed using the X-ray fluorescence (XRF) spectroscopy technique. Measurement was performed with a WD-XRF ZSX Primus II Rigaku spectrometer (Rh lamp).

2.3. Experimental setup

TW pyrolysis experiments were conducted on a micro scale and laboratory scale using a DT-FBR. Micro-scale pyrolysis investigation of TW was carried out using a pyrolysis–gas chromatography–mass spectrometry (Py-GC–MS) system to examine the composition of the products released during thermal and catalytic runs. The Py-GC–MS system was combined with a CDS Analytical micropyrolyser (model: 5200) coupled with Agilent Technologies GC (model: 7890B) and MS (model: 5977A). The pyrolysis process was conducted for three sample configurations: i) non-catalytic tyre waste pyrolysis, ii) catalytic pyrolysis in a layered system (wool/TW/catalyst/wool), and iii) catalytic pyrolysis (wool/TW and catalyst mix/wool). The weight of the sample for the TW pyrolysis process was approximately 0.6 mg ± 0.1 g. In turn, the samples for catalytic pyrolysis had a mass of 1.2 ± 0.1 (sum of the masses of tyre waste and catalyst with a catalyst-to-sample ratio of 1:1). The samples were placed in a quartz tube plugged on both sides with quartz wool and placed in a pyrolyser filament coil. All tests were carried out at constant temperature (i.e. 500 °C) under an inert atmosphere (He, grade: 6.0). The applied heating rate (that is, 100 °C/s) was set to be close to the estimated values for the DT-FBR. The samples were maintained at designated processing temperatures in the pyrolysis zone for 20 s. The experiments were carried out in the direct mode (analytes were transferred directly to the analyser). Analytes were separated using an Agilent HP-5MS capillary column (60 m × 0.25 mm × 0.25 μm). The temperature of the GC column oven was programmed as follows: (i) 40 °C for 7 min, (ii) 40–300 °C at a heating rate of 4 °C/min; and (iii) 300 °C for 10 min. MS spectra were interpreted based on the reference MS library (chemical base NIST14). Other details of the Py-GC–MS procedure can be found in work [34].

Laboratory-scale pyrolysis experiments were conducted in an electrically heated DT-FBR, as shown in Fig. 1. The TW particle size fraction (500–800 μm) was fed using a micro-feeder. The particles falling into the microfeeder chamber self-densified. After an hour of reactor operation, the microfeeder was opened to improve the loosening of the TW particles. Consequently, the mass feed rate decreased slightly over time (approximately 2 g less per hour of operation). The average feed rate was 14 g/h. The falling particles were rapidly heated by pre-heated pri-

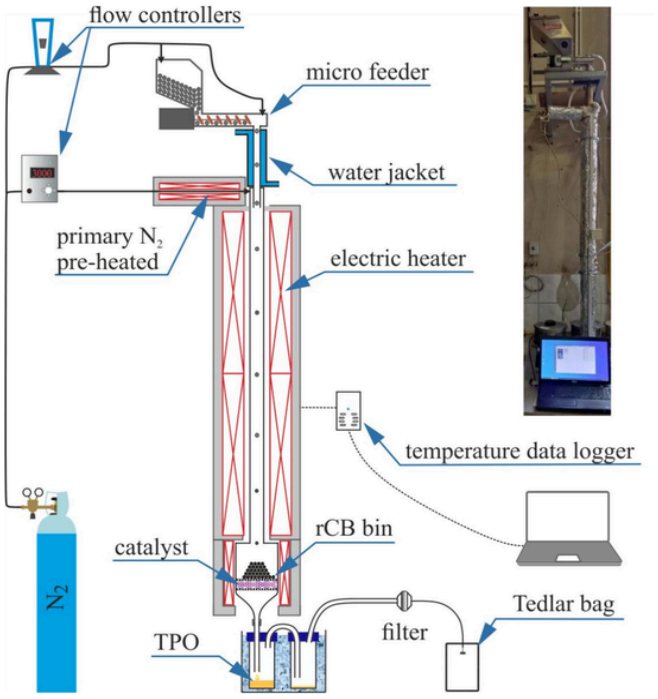

Fig. 1. Experimental pyrolysis set-up with the drop-tube–fixed-bed reactor.

mary nitrogen at 550 °C. The nitrogen flow rates were 1.5 (primary) and 0.5 L/min (secondary) measured at 20 °C and 101.3 kPa. The reactor tube was 2-m long with an internal diameter of 0.015 m. The double-zone heated reactor was monitored using five type-K thermocouples evenly spaced along the length of the reactor tube. The highest temperatures occurred in the middle of the 1-m heating zones and amounted to 580 °C. The temperatures measured every 0.5 m from the top of the reactor were 420, 580, 495, 580, and 430 °C. The average temperature of five thermocouples was assumed to be the pyrolysis temperature, which was about 500 °C. The estimated vapour residence time (VRT) in the reactor, based on the reactor dimensions and volumetric nitrogen flow rate, was 10.6 s. rCB was collected in a bin heated to 350 °C on a thin layer of wool. Maintaining this temperature prevented the condensation of oil vapours and sticking of rCB. In the case of catalytic pyrolysis, there was additional wool (under rCB wool) with 1 g of zeolite Y catalyst. The rCB bin was replaced with a new bin 1 h after the operation. The sample-to-catalyst ratio was 1:14. The catalyst temperature was equal to that of the rCB bin. The last part of the system was a gas cooler filled with ice, where the TPO was condensed. Non-condensed gases were collected in Tedlar bags to analyse the TPG composition using a gas chromatograph.

3. Results and discussion

Preliminary investigations included the TGA characterisation of tyre waste to evaluate the thermal degradation of the sample under a nitrogen atmosphere. This method allowed to estimate the optimal temperature for investigating the pyrolysis process using reactors on a micro and laboratory scale.

3.1. Tyre waste characteristic by thermogravimetric analysis

As shown in Fig. 2, three mass-loss stages are observed. Stage 1 is related to the initial degradation and decomposition of the TW sample resulting from the evaporation of volatile matter. The released volatiles may contain a mixture of moisture, oil, fabric, filler, and organic addi-

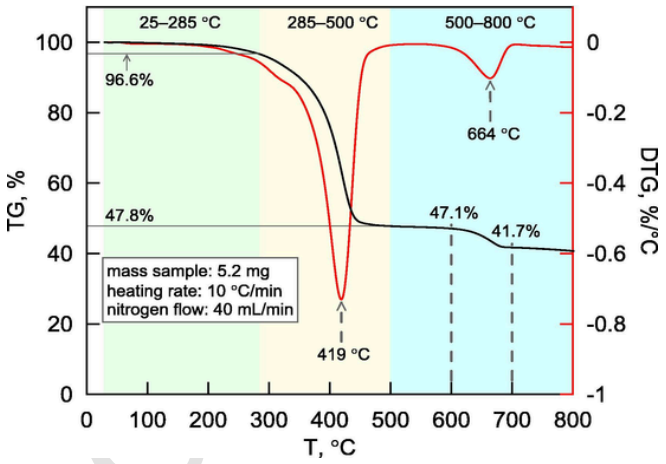

Fig. 2. Thermal analysis of the pyrolysis of tyre waste (TW).

tives [35]. The sample lost only 3.4 % of its initial mass. In the main pyrolysis process stage (stage 2) that extended in the temperature range of 285–500 °C, the maximum mass loss fell at the derivative thermogravimetry (DTG) peak at 419 °C, which may have corresponded to the degradation of rubber compounds (natural, butadiene, and styrene-butadiene rubbers) [36]. In the last stage, which took place in the temperature range of 500–800 °C the pyrolysis products were cracked, which showed good agreement with Chen et al. [37]. As the temperature increased from 500 to 800 °C, the percent masses of the solid residue were 47.8, 47.1, 41.7, and 40.7 %, respectively.

3.2. Pyrolysis products obtained in a micro-scale reactor

These studies were used to optimise the design of the drop-tube–fixed-bed reactor and analyse the potential catalytic effect of the zeolite Y. Herein, two approaches were studied: one in which the catalyst was mixed with TW and the other in which TW and catalysts were placed separately in layers. The pyrolytic decomposition of TW was investigated using pyrolysis–gas chromatography–mass spectrometry (Py-GC–MS). The total ion chromatograms (TIC) of the analytes released during the thermal and catalytic runs (both with mixed and layer systems) are shown in Fig. 3. Table S1 (see supplementary material) shows compounds that evolved during the thermal and catalytic runs. The peak numbers are marked in Fig. 3 and explained in Table S1. The conversion of TW without the addition of a catalyst (‘non-catalytic run’) is driven mainly by its thermal decomposition (thermal effect). Heating in the absence of oxygen reveals the depolymerisation and decomposition of organic macromolecules as building blocks of the tested material, generating reactive lower-molecular compounds that form gaseous and liquid fractions. As a result, compounds with wide molecular mass distributions can be observed. Thermal pyrolysis requires high temperatures and can result in low-quality products.

The addition of a catalyst to the reaction system provides an alternative route for the reaction with lower activation energy (e.g. promotion of the breaking of C–C bonds, determination of the length of the chains), and as a consequence, reduction of the decomposition temperature or shortening reaction time. However, the form of location of the catalyst (mixed with raw material versus layers) is crucial for its catalytic activity. Much more beneficial is the application of the layer system (‘catalytic run (layers)’) in which diffusion of the formed pyrolytic primary by-products into the structure of the catalyst is much easier. Such an approach reduces diffusion limitation and enhances catalyst efficiency. When the feedstock is mixed directly with the catalyst, the diffusion of formed pyrolytic products is much more limited. The catalyst is dispersed, and as a result, not all of the formed molecules can go

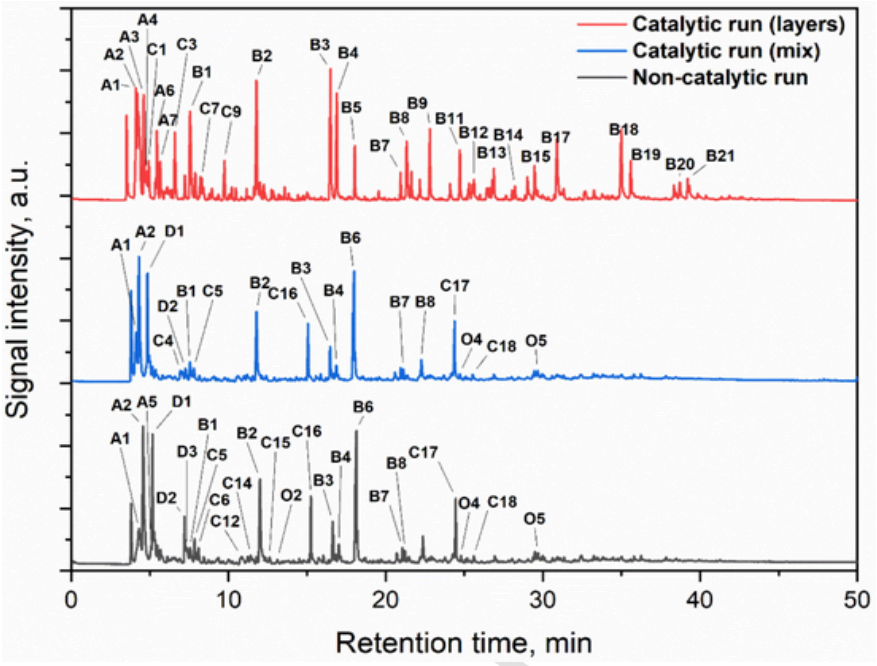

Fig. 3. TIC chromatograms of the thermal and catalytic pyrolysis of TW investigated through Py-GC–MS analysis (peak designations are explained in Table S1 in the supplementary material).

through the catalyst sites. Moreover, high-molecular compounds formed at the beginning of pyrolysis (with high diameters) can encounter strong diffusion resistance at acidic sites. Furthermore, some of the by-products can be highly reactive and undergo condensation, forming polyaromatic hydrocarbon structures and finally a secondary char. The residual matter is composed of residual organic matter ('depleted') and inorganic material. These residual fractions stay in the quartz tube and stick to the wall of the tube, as well as quartz wool. Thus, during pyrolysis, secondary char can be formed and stick to the surrounding catalyst (in the case of 'catalytic run (mix)') causing coke deposition at the catalyst sites and its fast deactivation. Liquid condensation and pore filling can also influence the significant decrease in the diffusion of reactant gases to the catalyst sites. Generally, it can lead to reduced (or even lack) catalyst efficiency in the case of the mixed approach.

In general, TW pyrolysis resulted in the evolution of a mixture of various compounds (>100 peaks). The TIC chromatograms exhibited mutual qualitative similarity, but some differences were observed depending on the system in which the catalyst was used. It can be seen that mixing the catalyst with the raw material resulted in limited catalytic activity (higher similarity of chromatograms). However, placing the catalyst in the layer resulted in a higher number and abundance of observed peaks, indicating higher zeolite activity.

To facilitate the analysis of the reaction mechanism pathways, the identified compounds were grouped as follows: (i) linear alkanes and alkenes; (ii) diene and triene hydrocarbons; (iii) cyclic hydrocarbons; (iv) aromatic hydrocarbons; (v) oxygen compounds; and (vi) unidentified compounds. The proportions of the respective groups in the thermal and catalytic runs are presented in Fig. 4. The yields of the presented groups of compounds were calculated as the ratio of the peak areas of all compounds to the total peak areas of all compounds in all groups (including the peak areas of the unidentified compounds). The products released during the pyrolytic decomposition of TW constituted a complex mixture of various hydrocarbons. Among the evolved moieties, various hydrocarbons were the dominant contributors, including aromatics, alkanes, alkenes, alkadienes, and cyclic hydrocarbons. In the

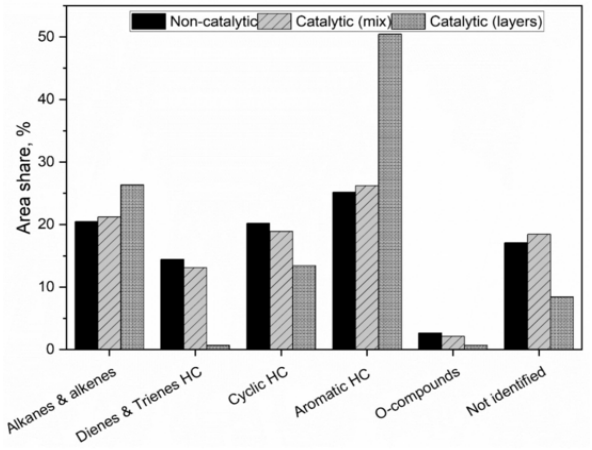

Fig. 4. Non-catalytic and catalytic pyrolysis of tyre waste.

case of purely thermal processes (lack of a catalyst), linear aliphatic hydrocarbons constituted 34.9 %, with a relatively high proportion of reactive alkadienes and alkatrienes (14.4 %). Cyclic and aromatic hydrocarbons were also present, with noticeable contributions of 20.2 % and 25.1 %, respectively. A minor proportion constituted oxygen compounds (2.7 %). Among the identified pyrolytic products, chain and isomer aliphatic compounds, as well as single- and multiple-ring structures, were identified. The major compounds in the analysed mixture were butene, pentene, cyclopentene, limonene, pentadiene, benzene, toluene, ethylbenzene, and styrene.

The composition of the resulting mixture was consistent with the data reported in the literature [38]. The catalytic pyrolysis over the zeolite Y resulted in noticeable changes in the composition of the released analytes. Generally, an increase in the contents of aromatics and alkanes was observed, along with a decrease in alkadienes, alkatrienes, and cyclic hydrocarbons. However, it is worth emphasising that the men-

tioned effect was only slight for the system with mixed TW and the catalyst, whereas it was pronounced for the layered system. For the latter, the proportions of aromatics and linear aliphatics increased to 50.5 % and 26.3 %, respectively. This agrees with the findings of Miandad et al. [30] who confirmed the preferred production of aromatic compounds over synthetic zeolites during the catalytic pyrolysis of tyre waste. The styrene component and polyisoprene rubber included in tyres, contribute mainly to the direct production of aromatic compounds [39]. However, other components of tyres (polybutadiene rubber, nylon, polyester, polypropylene, and polyethylene) can also contribute to the formation of aromatic compounds through secondary reactions of intermediate products [40].

Additionally, the deoxygenation effect was observed. The proportion of oxygen compounds decreased from 2.7 % for the thermal process to 0.7 % for the catalyst application in the layer system. The observed changes can be ascribed to the aromatisation of reactive aliphatic molecules (with multiple double bonds), that is, through Diels–Alder reactions or dehydrogenation reactions of the cyclic structures. Furthermore, the available alkadienes can react with alkenes to form aromatic structures. The identified peaks accounted for approximately 82–91 % of the total peak area in the resultant chromatograms.

3.3. Pyrolysis products obtained in a drop-tube–fixed-bed reactor

First, the functional groups of organic compounds in the catalyst and pyrolysis products were assessed using FT-IR analysis. The spectra of rCB and the used catalyst were compared with those of a TW sample and the raw catalyst. As a result, it was possible to better understand the changes that occur in the pyrolysis products.

3.3.1. Fourier transform infrared spectroscopy

Fig. 5a–c) show the spectra of TW, rCB, TPOs (TPO—pyrolysis oil from the non-catalytic process and TPO_cat—pyrolysis oil from the catalytic process), and the catalyst. The spectra were divided into single, double, triple, and fingerprint regions to facilitate the interpretation of the results. As shown in Fig. 5a), the spectrum of the TW sample included many vibrations, whereas the vibrations of the rCB sample were much smaller. The first absorption band of the TW sample at 3687 cm^{-1} was attributed to O–H stretching, which confirmed the presence of hydroxyl groups, such as alcohols and phenols [41]. The sources of C–H stretching vibrations at 2915 and 2849 cm^{-1} were alkanes [29]. The only vibration of an alkyne triple bond was that of C≡C at 2110 cm^{-1}. Three C = C stretching vibrations were also recorded at 1650, 1590, and 1542 cm^{-1} from alkenes, cyclic alkenes, and aromatics, respectively [42]. Most of the peaks were observed in the fingerprint region. The relative values of the bands at 1440, 1368, and 1083 cm^{-1} were assigned to $–CH_2–$, $–CH_3$, and Si–O, respectively [32]. Methylene and methyl groups were the elastomeric components. The asymmetric stretching vibration of Si–O–Si confirmed that, in addition to rubber and carbon black, TW also contained SiO_2 [43]. The addition of SiO_2 to tyres improved their elasticity. The last three vibrations in the fingerprint region represented carbon black (at 1012 cm^{-1}), aromatic compounds C–H (at 683 cm^{-1}), and sulphur compounds S–S (at 530 and 459 cm^{-1}). S–S bridges are formed during tyre manufacturing [32]. TW

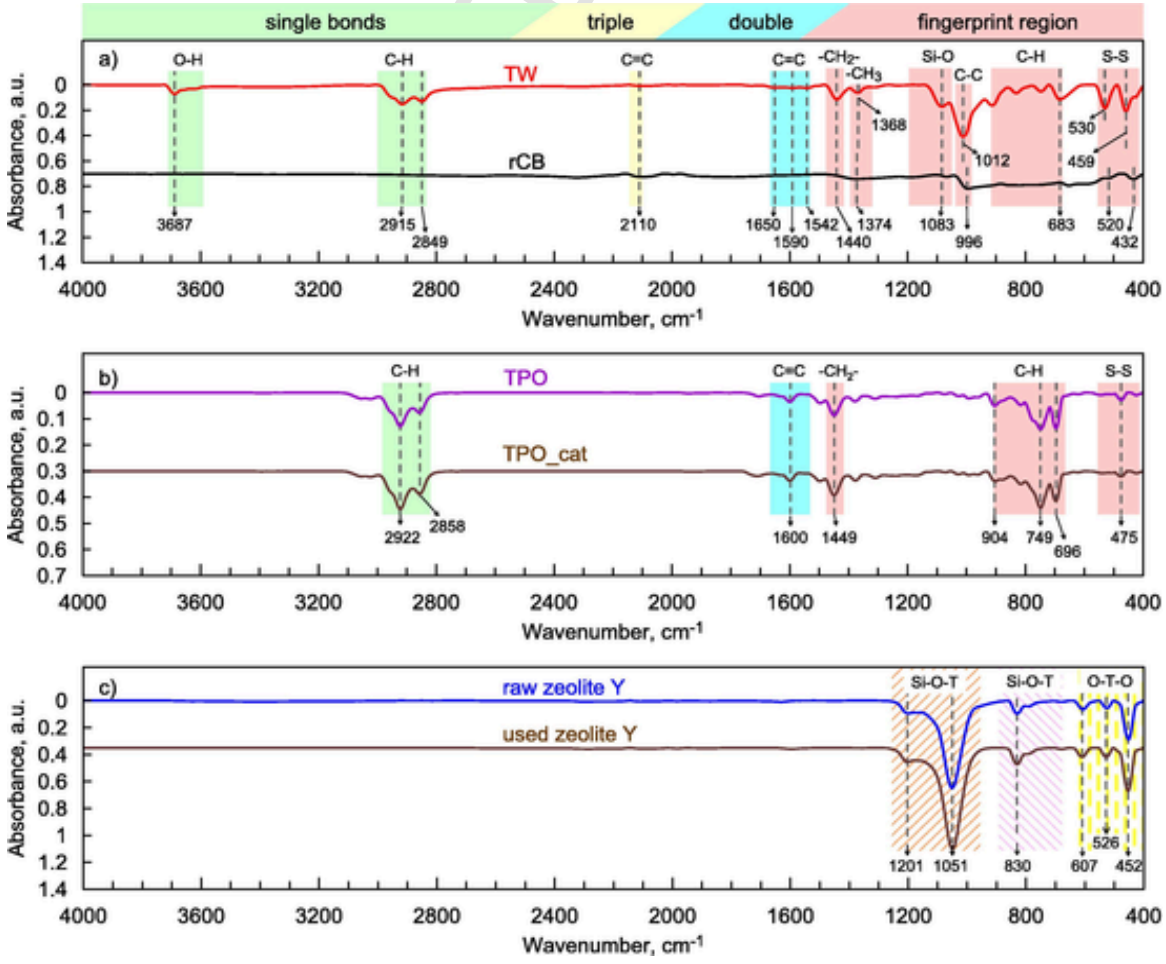

Fig. 5. FT-IR spectra for: a) TW and rCB, b) TPOs, and c) catalyst before and after pyrolysis.

pyrolysis decreased the vibrations assigned to the elastomeric, carbon black, and sulphur components of rCB. Energy of 272.8 kJ/mol is required to break a single bond between S atoms and 377.4 kJ/mol to break the C–C bond [44].

Fig. 5b) illustrates the FT-IR spectra of TPO and TPO_cat. Absorbance peaks associated with C–H bonds were observed for both TPOs at 2922, 2858, 904, 749, and 696 cm^{-1}. The strongest absorbance in the C–H stretching zone occurred at 2922 and 749 cm^{-1}. In turn, Fernández-Berridi et al. [45] suggested that the vibrations at 749 and 696 cm^{-1} were caused by aromatic C–H groups of styrene. TPO_cat was characterised by a weaker peak at 696 cm^{-1}. This vibrational bending may be associated with the open-chain hydrocarbons containing four or more CH_2 groups [44]. The presence of alkenes was confirmed by the small peak at 1600 cm^{-1} (C = C). Finally, small vibrations from the S-S bridge indicated that part of the sulphur was transferred to the TPOs. The FT-IR spectra of the zeolite Y catalyst (raw and used) catalysts are shown in Fig. 5c). zeolite Y (faujasite structure) is a compound of crystalline aluminosilicates of SiO_4^{4-} and AlO_4^{3-} bonded together. The vibrations of the zeolite Y lattice were observed in the spectral region below 1250 cm^{-1}. Si–O–T was assigned to internal and external asymmetrical stretching vibrations at 1201 and 1051 cm^{-1}, respectively, and symmetrical stretching vibrations at 830 cm^{-1}. Double vibrations of the polyhedral external ring were found in the secondary building unit at 607 and 526 cm^{-1}. Finally, the range at 452 cm^{-1} was attributed to the structure-insensitive O–T–O bending modes. The FT-IR spectra shown in Fig. 5c) are very close to the zeolite Y absorption peaks reported by Król et al. [46].

The lack of significant changes in the spectra of the raw and used catalysts was due to the low temperature of the bed in which the catalysts were placed. Although carbon vibrations were not found in the catalyst spectrum, the possibility of coke deposition on zeolite Y is investigated in the next section.

3.3.2. Yields

The yields of the pyrolysis products obtained in the DT-FBR were compared with those reported in the literature for various reactors and are presented in Table 3. The VRTs in the hot zone of the reactors ranged from 0.5 to 30 s. The grinding of ELTs for pyrolysis involves the removal of steel; therefore, the main pyrolysis products were rCB, TPO, and TPG. The reactors are listed in order of decreasing TPO yields. Based on a review of available literature, ELTs pyrolysis using a drop-tube reactor has been performed only once [23]. Additionally, the TPO yield was the lowest among those listed in Table 3. The catalytic pyrolysis of ELTs over zeolite Y has been extensively investigated. Most studies were conducted in fixed-bed reactors at low heating rates (HR). Catalysts have been employed to improve the quality of TPO by reducing their hydrocarbon content. The product yields obtained in this work are presented with a deviation (±) due to the variability in the TW feeding during the experiment, as explained in the experimental procedure. For the catalytic and non-catalytic pyrolysis, the rCB yields were the same (40.8 %). This resulted in noncontact between rCB and the catalyst; thus, the catalyst did not influence the rCB yield. The high heating rate of the sample in the DT-FBR reactor allowed to achieve the rCB yield, which was observed in the TGA after reaching 800 °C. The TPO yield obtained from non-catalytic pyrolysis of 38 wt% was satisfactory compared with the other results listed in Table 3. This is a particularly good result when evaluating the ash content of the feedstock (which limits the TPO yield). In this study, TW contained up to 21.4 % ash, whereas the ELT values from the literature were 2.14 [27], 3.3 % [16], 4.9 % [17], 5.9 and 6.5 % [19] and 22.80 [31]. Therefore, it seems reasonable to use the DT-FBR for tyre waste pyrolysis. The pyrolysis of TW over zeolite Y reduced the TPO yield by 3 wt%. This can be considered as a minor loss if the quality of the TPO is improved by reducing the oxygen content.

3.3.3. Composition

Fig. 6a–f) show the elemental and chemical compositions of rCB, TPOs, and zeolite Y (catalyst after 1 h of pyrolysis) expressed in weight percentages and the composition of TPGs in volume percentage. The rCB yields for non-catalytic and catalytic pyrolysis were the same because the catalyst was located below the rCB bed. As a result, only the TPO and TPG yields were affected. rCB contained a large amount of ash (49.8 %). Based on the calculations and considering the 40.8 % yield of rCB and its ash content, the theoretical ash content of TW was 20.3 %. This value is close to the experimental results shown in Table 2 (21.4 %). Typically, rCB from ELTs has a low ash content that does not exceed 16 % [47]. However, rCBs with high ash contents of up to 55.1 % have also been reported [27]. The carbon and hydrogen contents of rCB were 39.3 % and 1.80 %, respectively. The high ash content and the presence of 1.3 % sulphur in rCB limit its applicability. Therefore, rCB must be treated to obtain commercially available carbon black with > 95 % C, <1% S, and < 1 % ash [9]. Demineralisation processes such as leaching can be carried out for TW before pyrolysis or for rCB. The HHV of TPO was calculated using the Dulong formula:

$$HHV = \frac{\left[338.2 \bullet C + 1442.8 \bullet \left(H - \frac{O}{8}\right)\right]}{1000}, MJ/kg \quad (1)$$

where C, H, and O are the percentages of carbon, hydrogen, and oxygen, respectively.

As reported by Ferdinand et al. [48], Dulong's formula is suitable for reflecting the results of HHV measurements of pyrolysis oils from various feedstocks. The HHVs of TPO (Fig. 6b)) and TPO_cat (Fig. 6e)) were 40.1 and 41.0 MJ/kg, respectively. The positive effect of catalytic pyrolysis was the reduction in the oxygen content of TPO_cat. These TPOs have the potential to replace diesel fuels because their HHVs are similar. Additionally, a chromatographic analysis of organic compounds present in TPO and TPO_cat was performed (see supplementary material Table S2).

Fig. 6c) and 6f) show the nitrogen-free compositions of the pyrolytic gas (TPGs). Gaseous products of the process were generated during thermal decomposition in an anaerobic atmosphere. The influence of high temperature (500 °C) during the pyrolysis of tyres results in simpler chemical compounds originating from the breakdown of complex organic substances. In the process of heating organic materials, typical combustion byproducts like carbon monoxide (CO) and carbon dioxide (CO_2) are produced and were identified in the obtained pyrolytic gas. The main chemical compounds in obtained gas were C_2H_4, CH_4 and H_2. The use of a catalyst reduced the hydrogen content and all hydrocarbons present in TPG_cat. However, the reduction was more significant for heavy hydrocarbons (from 5.9 % to 4.2 % for C_4H_8) than that for light hydrocarbons (from 27.6 % to 27.2 % for CH_4). TPG_cat was richer, with 1.3 % CO and 4.2 % CO_2.

Muenpol et al. [49] confirmed that the use of various zeolites in the pyrolysis of ELTs reduced the CH_4 and C_2H_6 contents of the gas. A positive correlation was also found between the decrease in the content of gaseous components in the TPGs and the sample-to-catalyst ratio [15]. The exception was the increase in the CO_2 content in TPG_cat. Generally, the compositions of TPGs obtained by different types of reactors are similar. TPGs typically comprise CH_4, H_2, CO, CO_2, olefins (C_2H_4 and C_3H_6), paraffins (C_2H_6 and C_3H_8), and C_4. When evaluating only the alkanes in the TPG, CH_4 was the most abundant during pyrolysis in the CFBR [16], C_2H_4 in the FBR [11], and C_2H_6 in the CSBR [50].

The rCB bin temperature of 350 °C prevented TPO condensation. At this temperature, coke is formed in the catalyst bed. As shown in Fig. 6d), the coke contained 6.6 % C and 1.25 % H in the catalyst after 1 h of pyrolysis.

Table 3
Review of the literature on the product yields from end-of-life tyre pyrolysis (without a catalyst and over zeolite Y catalyst) carried out in various reactors and operating conditions, where T—pyrolysis temperature, PS—particle size, FR—feed rate, VTR—vapour residence time, HR—heating rate, S/C—sample-to-catalyst ratio, and T_{cat}—catalyst temperature.

Pyrolysis without a catalyst

Type of reactor	T, °C	PS, mm	FR, g/min	VRT, s	HR, °C/s	rCB, wt.%	TPO, wt.%	TPG, wt.%	Refs.
CSBR	425	2.8–3.3	1.3	0.5	1000–10,000	37.9	58.4	3.7	[17]
	475					35.9	58.2	5.9	
	575					35.9	54.0	10.1	
FLBR	598	0.8–1.6	50	2.6	nd*	30.0	50.0	20.0	[14]
AUR	500	2–4	66.7	30	0.17	41[a]	41[a]	18[a]	[19]
	500					38[b]	50[b]	12[b]	
	600					40[a]	31[a]	29[a]	
	600					35[b]	40[b]	25[b]	
CFLBR	500	0.32	83.3	5	1000	21.7	46.4	28.6	[16]
RKR	450	13–15	200–250	nd*	nd*	43.9	43.0	13.1	[21]
	500					41.3	45.1	13.6	
	550					39.9	44.6	15.5	
	600					39.3	42.7	18.0	
	650					38.8	42.9	18.3	
DT-FBR	500	0.5–0.8	0.23	11	500	40.8 ± 2.1	38.0 ± 3.3	21.2 ± 1.9	Present study
FBR	600	1–3	1.33	nd*	nd*	40.39	33.45	26.16	[10]
						37.29	35.48	27.23	
						35.29	35.50	29.21	
DTR	450	4	0.5	nd*	nd*	35.3	37.8	26.9	[23]
	750					37.0	10.9	51.4	
	1000					37.7	< 0.01	37.2	

Pyrolysis over a zeolite Y catalyst

Type of reactor	T, °C	T_{cat}, °C	S/C	PS, mm	FR, g/min	VRT, s	HR, °C/s	rCB, wt.%	TPO, wt.%	TPG, wt.%[c]	Refs.
FLBR	500	450	1	1.0–1.4	3.6–3.8	nd*	nd*	42.7	46.2	11.1	[15]
	500	500	1					42.8	45.9	11.3	
	500	550	1					42.8	43.9	13.3	
	500	600	1					42.2	42.2	16	
FBR	500	430	1	1.0–1.4	nd*	nd*	0.17	37.7	38.6	16.3	[11]
		470	1					37.7	38.6	16.4	
		500	1					37.8	36.0	19.2	
		530	1					37.8	35.2	19.4	
		600	1					38.0	32.2	21.6	
DT-FBR	500	350	14[d]	0.5–0.8	0.23	11	500	40.8 ± 2.1	35.0 ± 2.5	20.2 ± 1.6	Present study
FBR	500	400	4	8–10	nd*	nd*	0.17	36.5	31.6	31.48	[12]
			2					36.1	23.3	40.7	
			1.3					36.7	19.1	44.0	
			1					36.6	13.9	49.3	
FBR	500	350	2	1–3	nd*	nd*	0.17	45.0[e]	38.4[e]	8.3[e]	[13]
CSBR	500	500	0.13	nd*	2	nd*	nd*	35.7	61.8	2.5	[18]

* nd—no data, a—passenger car tyres, b—commercial truck tyres, c—catalyst coke completes the balance at 100 %, d—in relation to 1 h of pyrolysis, and e—mole percent.

3.3.4. Thermal analysis of tyre pyrolysis oil combustion

Fig. 7a) and 7b) show the TG and DTG curves of the combustion of TPOs in a temperature range between 30 and 700 °C. The oxidation of TPOs can be divided into three stages based on the DTG curves. Other researchers observed similar stages [51,52]. Low-temperature oxidation (LTO) is the first stage that occurs, from 30 to 350 °C (5 °C/min), 400 °C (10 °C/min), and 431 °C (20 °C/min) for TPO, and 350 °C (5 °C/min), 359 °C (10 °C/min), and 426 °C (10 °C/min) for TPO_cat. Moreover, all peaks in the TPOs from catalytic pyrolysis were observed at higher temperatures. Temperature peaks were present at 155, 191, and 209 °C for TPO, and 175, 197 and 220 °C for TPO_cat for heating rates of 5, 10, and 20 °C/min, respectively. The increase in the heating rate influenced the kinetics of the combustion process, which was reflected in the shift of the temperature peaks towards higher values [53]. The evaporation of highly volatile hydrocarbons resulted in a loss of 77.2–84.2 % of the sample weight, making it the main stage. This indicated the significant presence of light hydrocarbons in TPO and TPO_cat.

The second stage, called mid-temperature oxidation (MTO), was characterised by a number of lower-intensity peaks. The driving force was the cracking of high-molecular-weight compounds and oxidation of the LTO residue. The mass loss of MTO ranged from 5 to 10 %. MTO is considered as a transition stage from low-temperature to high-temperature oxidation (HTO), where the presence of aromatic compounds and resins is an important factor influencing the rate of mass loss [54]. In MTO, one of the intermediates is coke, which is oxidised during HTO. HTO is the final stage of TPO combustion, and the MTO residue is oxidised to CO_2 and H_2O. According to the elemental analyses of the TPOs (Fig. 6b and 6e), approximately 1.5 % sulphur and 1 % nitrogen were present in the TPOs.

These elements are oxidised in the HTO stage and form pollutants, such as NO and SO_2. Similar to the LTO stage, the heating rate determined the peak temperature corresponding to the maximum mass loss. The burnout of TPO and TPO_cat occurred above 650 °C at a heating rate of 20 °C/min.

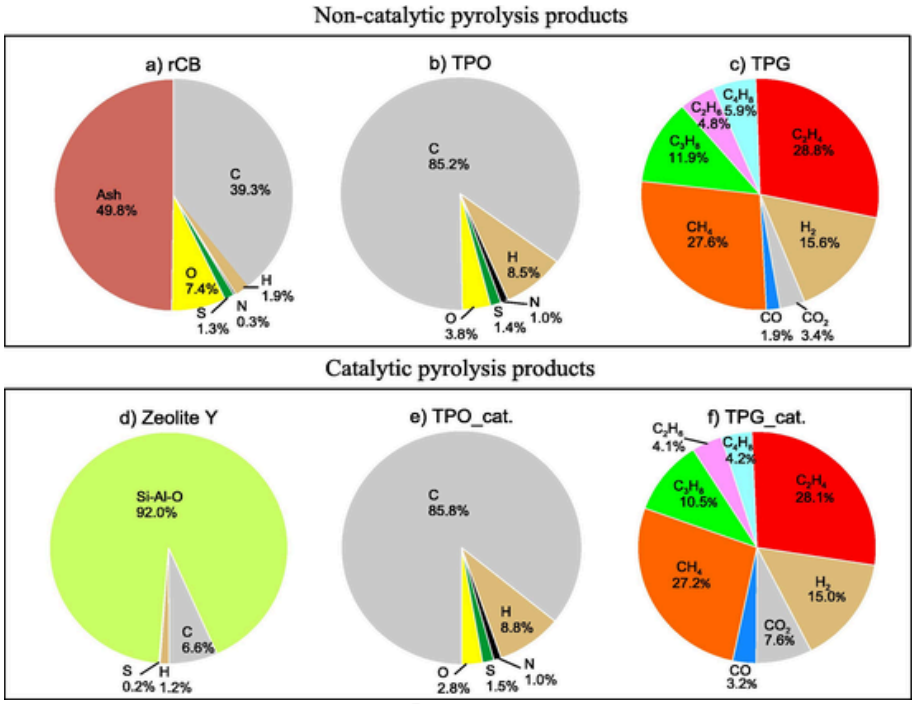

Fig. 6. Chemical composition of products from a-c) non-catalytic and a, d-f) catalytic pyrolysis of tyre waste.

3.3.5. Potential of ash from raw carbon black as a catalytic carrier

Attempts have been made to produce catalysts using various solid fuels. The total gas yield from biomass pyrolysis can be significantly increased from 40 % (pyrolysis without a catalyst) to 60 % when RDF ash is used as a catalyst [55]. Table 4 shows the compositions of rCB ash and zeolite Y determined by XRF. The presence of zinc, sodium, and aluminium oxide, among others, in the ash makes it reasonable to use tyre ash as a catalyst support material for biomass thermal conversion. Moreover, the decomposition of methane over biomass fly ash enhances hydrogen production [56]. The Brunauer-Emmett-Teller specific surface area of the zeolite Y catalyst was significantly higher than that of rCB ash, at 780 and 66.74 m^2/g, respectively. The surface area and porosity of rCB ash may not be optimized for catalyst support applications [57]. High surface area and porosity are desirable characteristics for catalyst supports as they provide more active sites for catalytic reactions. However, rCB ash may not possess these properties to the same extent as other commercially available catalyst supports. Based on the SiO_2 and Al_2O_3 contents, the molar silica-to-alumina ratio (SAR) was determined. The SAR values were 111.8 and 26.3 for rCB ash and zeolite Y, respectively. The SAR is reversibly associated with zeolite acidity and, therefore, the activity of the catalyst [58]. Zeolites with a wide range of SAR of 2 to 1500 are available [59]. An increase in the SAR led to a decrease in the total acidity of the catalyst [60]. This indicates a direct correlation between the increase in the SAR value and the decrease in cracking reaction activity. However, this relationship indicates the possibility of actively adjusting the silica-to-alumina ratio to obtain specific process products [61]. The results of the FT-IR analysis indicated a higher yield of hydrocarbon compounds in the C5–C12 range for pyrolysis without the presence of a catalyst owing to the high SAR value for rCB. Moreover, using rCB ash as a catalyst support material has several potential limitations and challenges that could affect its overall effectiveness and applicability. Firstly, rCB ash composition can vary depending on the source of the carbon black and the combustion process used to produce it. This variability in composition can lead to inconsistencies in the material properties, affecting its ability to support catalysts uniformly [62]. Depending on the production process and source materials, rCB ash may contain impurities or contaminants that could leach into the reaction environment and interfere with the catalytic process. Contaminants such as heavy metals or organic compounds may adversely affect the selectivity and efficiency of the catalyst [63]. The mechanical stability of rCB ash may be insufficient to withstand the harsh conditions often encountered in catalytic processes, such as high temperatures, pressures, and mechanical agitation [64]. This could result in the degradation or fragmentation of the support material over time, leading to catalyst deactivation or loss of activity. Addressing these limitations and challenges require further research and development to optimize the properties of rCB ash as a catalyst support material and demonstrate its effectiveness and reliability in practical applications.

The introduction of zeolite Y to the process led to the decomposition of these compounds. It should also be noted that high SAR lead to high catalyst stability and product yields [59]. As shown in Fig. 4, in the case of a process without a catalyst or when the catalyst was mixed directly with the feedstock, high yields of hydrocarbons and aromatic compounds were obtained. Furthermore, a lower concentration of acidic sites (higher SAR value) lowered the coke deposition rate. This leads to the maintenance of catalyst activity for a longer period [65]. These results demonstrate the high potential of rCB to catalyse the pyrolysis process and direct the process toward specific end products.

4. Conclusions

In this study, a tyre waste pyrolysis process was experimentally investigated at 500 °C using a pyrolysis–gas chromatography–mass spectrometry (Py-GC–MS) and using a drop-tube–fixed-bed reactor (DT-FBR). The tyre waste contained a high ash content of 21.4 %, which favoured the production of raw carbon black, as confirmed by the thermal analysis of the sample.

On the basis of experiments performed using a Py-GC–MS, it was observed that the method of adding a catalyst for pyrolysis (catalyst mixed with tyre waste or arranged in layers) was essential for its catalytic activity. Using a layered system is significantly more advantageous be-

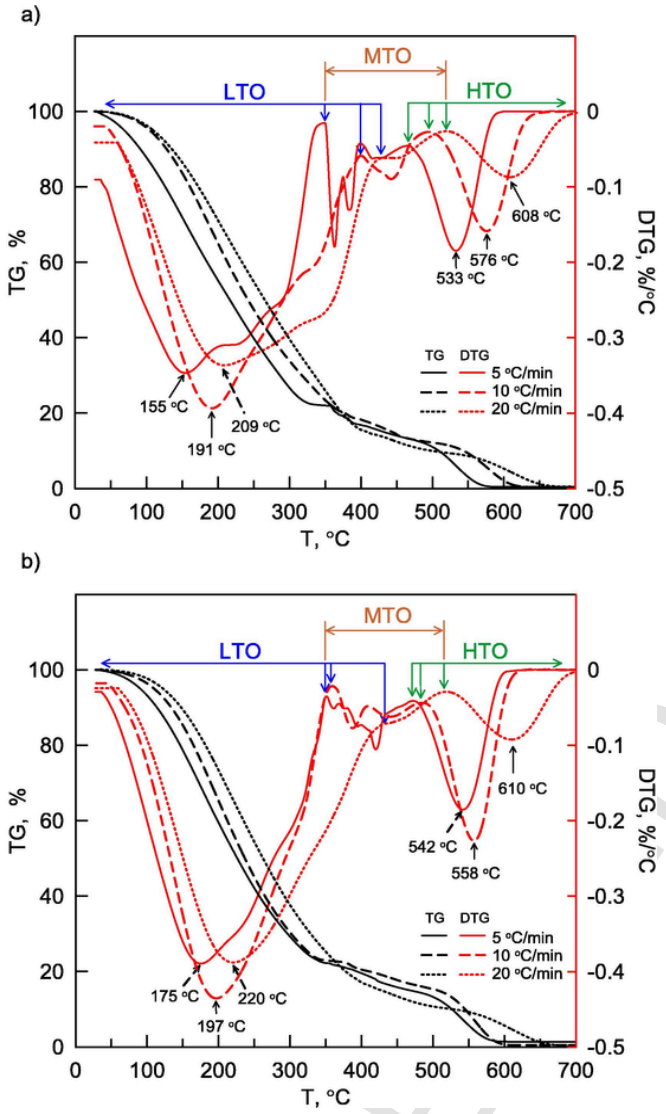

Fig. 7. Thermal analysis of the combustion process of tyre pyrolysis oils obtained from a) non-catalytic and b) catalytic processes.

cause it facilitates the diffusion of pyrolytic primary products into the catalyst's structure. The detailed identification of the formed compounds indicated a 20 % increase in the production of aromatic hydrocarbons when the tyre waste and catalyst were layered.

From the DT-FBR, the main pyrolysis product was raw carbon black, with a yield of 40.8 % (for both catalytic and non-catalytic pyrolysis). During pyrolysis without a catalyst, a 38 % yield of tyre pyrolysis oil was obtained. The use of the catalyst decreased the oil yield by 35 %. In addition, the catalytic pyrolysis oil contained less oxygen. The oil obtained from catalytic pyrolysis was completely burned at a temperature lower than that obtained from noncatalytic pyrolysis, as shown by the TGA. When assessing the tyre pyrolysis gas, the catalyst reduced the contents of all hydrocarbons and hydrogen at the expense of increasing the contents of CO and CO_2.

CRediT authorship contribution statement

Wojciech Jerzak: Writing – review & editing, Writing – original draft, Visualization, Software, Resources, Methodology, Investigation, Conceptualization. **Mariusz Wądrzyk:** Writing – original draft, Validation, Investigation, Formal analysis. **Małgorzata Sieradzka:** Writing – original draft, Validation, Resources, Investigation. **Aneta Magdziarz:** Writing – original draft, Supervision, Project administration, Investigation, Funding acquisition, Writing – review & editing.

Table 4
Chemical composition of rCB ash and zeolite Y.

Component	rCB ash	zeolite Y
	Content, wt.%	
Na_2O	1.09	0.04
MgO	0.12	–
Al_2O_3	1.36	6.05
SiO_2	89.59	93.74
P_2O_5	0.04	–
SO_3	0.90	0.09
Cl	0.05	–
K_2O	0.13	–
CaO	0.71	–
TiO_2	0.10	0.02
Fe_2O_3	1.05	0.02
CuO	0.08	–
ZnO	4.51	–
ZrO_2	0.10	0.02
Other	0.17	0.02

Declaration of competing interest

The authors declare that they have no known competing financial interests or personal relationships that could have appeared to influence the work reported in this paper.

Data availability

No data was used for the research described in the article.

Acknowledgement

This research was funded by the National Science Centre of Poland [grant no. 2020/39/B/ST8/00883].

A shortened version of this research was presented at the 18th Sustainable Development of Energy, Water, and Environment Systems (SDEWES) Conference in Dubrovnik, Croatia, September 24–29, 2023. The title of the conference paper was "Catalytic and non-catalytic pyrolysis of tyre wastes".

Appendix A. Supplementary material

Supplementary data to this article can be found online at https://doi.org/10.1016/j.enconman.2024.118642.

References

[1] Afash H, Ozarisoy B, Altan H, Budayan C. Recycling of tire waste using pyrolysis: an environmental perspective. Sustain 2023;15:14178. https://doi.org/10.3390/su151914178.

[2] The European Tyre & Rubber Manufacturers Association. In Europe 95% of all End of Life Tyres were collected and treated in 2019. 2021. https://www.etrma.org (accessed June 15, 2023).

[3] López F.A, Centeno T.A, Alguacil F.J, Lobato B, Urien A. The GRAUTHERMIC-tyres process for the recycling of granulated scrap tyres. J Anal Appl Pyrol 2013;103:207–15. https://doi.org/10.1016/j.jaap.2012.12.007.

[4] Kumar Singh R, Ruj B, Jana A, Mondal S, Jana B, Kumar Sadhukhan A, et al. Pyrolysis of three different categories of automotive tyre wastes: product yield analysis and characterization. J Anal Appl Pyrol 2018;135:379–89. https://doi.org/10.1016/j.jaap.2018.08.011.

[5] Taleb D.A, Hamid H.A, Deris R.R.R, Zulkifli M, Khalil N.A, Ahmad Yahaya A.N. Insights into pyrolysis of waste tire in fixed bed reactor: thermal behavior. Mater Today: Proc 2020;31:178–86. https://doi.org/10.1016/j.matpr.2020.01.569.

[6] Kaminsky W, Sinn H. Pyrolysis of plastic waste and scrap tires using a fluidized-bed process in "Thermal Conversion of Solid Wastes and Biomass", copyright. ACS Symp Ser 1980. https://doi.org/10.1021/bk-1980-0130.fw001.

[7] Bowles A.J, Fowler G.D. Assessing the impacts of feedstock and process control on pyrolysis outputs for tyre recycling. Resour Conserv Recycl 2022;182:106277. https://doi.org/10.1016/j.resconrec.2022.106277.

[8] Jerzak W, Reinmöller M, Magdziarz A. Estimation of the heat required for intermediate pyrolysis of biomass. Clean Techn Environ Policy 2022;24:3061–75. https://doi.org/10.1007/s10098-022-02391-1.

[9] Gao N, Wang F, Quan C, Santamaria L, Lopez G, Williams P.T. Tire pyrolysis char: processes, properties, upgrading and applications. Prog Energy Combust Sci 2022;93:101022. https://doi.org/10.1016/j.pecs.2022.101022.

[10] Chen G, Sun B, Li J, Lin F, Xiang L, Yan B. Products distribution and pollutants releasing characteristics during pyrolysis of waste tires under different thermal process. J Hazard Mater 2022;424. https://doi.org/10.1016/j.jhazmat.2021.127351.

[11] Williams P.T, Brindle A.J. Catalytic pyrolysis of tyres: influence of catalyst temperature. Fuel 2002;81:2425–34. https://doi.org/10.1016/S0016-2361(02)00196-5.

[12] Boxiong S, Chunfei W, Cai L, Binbin G, Rui W. Pyrolysis of waste tyres: The influence of USY catalyst/tyre ratio on products. J Anal Appl Pyrol 2007;78:243–9. https://doi.org/10.1016/j.jaap.2006.07.004.

[13] Khalil U, Vongsvivut J, Shahabuddin M, Priya S, Chakravartula S, Bhattacharya S. A study on the performance of coke resistive cerium modified zeolite Y catalyst for the pyrolysis of scrap tyres in a two-stage fixed bed reactor. Waste Manag 2020;102:139–48. https://doi.org/10.1016/j.wasman.2019.10.029.

[14] Kaminsky W, Mennerich C, Zhang Z. Feedstock recycling of synthetic and natural rubber by pyrolysis in a fluidized bed. J Anal Appl Pyrol 2009;85:334–7. https://doi.org/10.1016/j.jaap.2008.11.012.

[15] Williams P.T, Brindle A.J. Fluidised bed pyrolysis and catalytic pyrolysis of scrap tyres. Environ Technol (United Kingdom) 2003;24:921–9. https://doi.org/10.1080/09593330309385629.

[16] Dai X, Yin X, Wu C, Zhang W, Chen Y. Pyrolysis of waste tires in a circulating fluidized-bed reactor. Energy 2001;26:385–99. https://doi.org/10.1016/S0360-5442(01)00003-2.

[17] Alvarez J, Lopez G, Amutio M, Mkhize N.M, Danon B, van der Gryp P, et al. Evaluation of the properties of tyre pyrolysis oils obtained in a conical spouted bed reactor. Energy 2017;128:463–74. https://doi.org/10.1016/j.energy.2017.03.163.

[18] Olazar M, Aguado R, Arabiourrutia M, Lopez G, Barona A, Bilbao J. Catalyst effect on the composition of tire pyrolysis products. Energy Fuel 2008;22:2909–16. https://doi.org/10.1021/ef8002153.

[19] Sanchís A, Veses A, Martínez J.D, López J.M, García T, Murillo R. The role of temperature profile during the pyrolysis of end-of-life-tyres in an industrially relevant conditions auger plant. J Environ Manage 2022;317:115323. https://doi.org/10.1016/j.jenvman.2022.115323.

[20] Campuzano F, Cardona-Uribe N, Agudelo A.F, Sarathy S.M, Martínez J.D. Pyrolysis of waste tires in a twin-auger reactor using CaO: assessing the physicochemical properties of the derived products. Energy Fuel 2021;35:8819–33. https://doi.org/10.1021/acs.energyfuels.1c00890.

[21] Li S.Q, Yao Q, Chi Y, Yan J.H, Cen K.F. Pilot-scale pyrolysis of scrap tires in a continuous rotary kiln reactor. Ind Eng Chem Res 2004;43:5133–45. https://doi.org/10.1021/ie030115m.

[22] Tian X, Wang K, Shan T, Li Z, Wang C, Zong D, et al. Study of waste rubber catalytic pyrolysis in a rotary kiln reactor with spent fluid-catalytic-cracking catalysts. J Anal Appl Pyrol 2022;167:105686. https://doi.org/10.1016/j.jaap.2022.105686.

[23] Conesa J.A, Martín-Gullón I, Font R, Jauhiainen J. Complete study of the pyrolysis and gasification of scrap tires in a pilot plant reactor. Environ Sci Tech 2004;38:3189–94. https://doi.org/10.1021/es034608u.

[24] Zhang G, Chen F, Zhang Y, Zhao L, Chen J, Cao L, et al. Properties and utilization of waste tire pyrolysis oil: a mini review. Fuel Process Technol 2021;211:106582. https://doi.org/10.1016/j.fuproc.2020.106582.

[25] Wang F, Gao N, Quan C. Effect of hot char and steam on products in waste tire pressurized pyrolysis process. Energy Convers Manag 2021;237:114105. https://doi.org/10.1016/j.enconman.2021.114105.

[26] Wang F, Quan C, Liu H, Lang L, Yuan H, Yin X, et al. Energy and exergy analysis based on an energy saving process of waste tires pressurized catalytic reforming. Energy Convers Manag 2023;289:117191. https://doi.org/10.1016/j.enconman.2023.117191.

[27] Wang M, Zhang L, Li A, Irfan M, Du Y, Di W. Comparative pyrolysis behaviors of tire tread and side wall from waste tire and characterization of the resulting chars. J Environ Manage 2019;232:364–71. https://doi.org/10.1016/j.jenvman.2018.10.091.

[28] Wądrzyk M, Janus R, Rządzik B, Lewandowski M, Budzyń S. Pyrolysis oil from scrap tires as a source of fuel components: manufacturing, fractionation, and characterization. Energy Fuel 2020;34:5917–28. https://doi.org/10.1021/acs.energyfuels.0c00265.

[29] Wang Z, Wu M, Chen G, Zhang M, Sun T, Burra K.G, et al. Co-pyrolysis characteristics of waste tire and maize stalk using TGA. FTIR and Py-GC/MS analysis Fuel 2023;337:127206. https://doi.org/10.1016/j.fuel.2022.127206.

[30] Miandad R, Barakat M.A, Rehan M, Aburiazaiza A.S, Gardy J, Nizami A.S. Effect of advanced catalysts on tire waste pyrolysis oil. Process Saf Environ Prot 2018;116:542–52. https://doi.org/10.1016/j.psep.2018.03.024.

[31] Rećko K. Laboratory research on the possibility of producing fuels from municipal sewage sludge, rubber waste and biomass. Annu Set Environ Prot 2020;22:680–92.

[32] Colom X, Faliq A, Formela K, Cañavate J. FTIR spectroscopic and thermogravimetric characterization of ground tyre rubber devulcanized by microwave treatment. Polym Test 2016;52:200–8. https://doi.org/10.1016/j.polymertesting.2016.04.020.

[33] Wang F, Gao N, Quan C, López G. Investigation of hot char catalytic role in the pyrolysis of waste tires in a two-step process. J Anal Appl Pyrol 2020;146:104770. https://doi.org/10.1016/j.jaap.2019.104770.

[34] Wądrzyk M, Janus R, Lewandowski M, Magdziarz A. On mechanism of lignin decomposition – investigation using microscale techniques: Py-GC-MS. Py-FT-IR and TGA Renew Energy 2021;177:942–52. https://doi.org/10.1016/j.renene.2021.06.006.

[35] Rijo B, Soares Dias A.P, Wojnicki Ł. Catalyzed pyrolysis of scrap tires rubber. J Environ Chem Eng 2022;10. https://doi.org/10.1016/j.jece.2021.107037.

[36] Wu B, Liu B, Yuwen C, Bao R, Zhang T, Zhang L. Microwave preparation of porous graphene from wasted tires and its pyrolysis behavior. Waste Biomass Valoriz 2023;14:1969–78. https://doi.org/10.1007/s12649-022-01955-y.

[37] Chen J, Ma X, Yu Z, Deng T, Chen X, Chen L, et al. A study on catalytic co-pyrolysis of kitchen waste with tire waste over ZSM-5 using TG-FTIR and Py-GC/MS. Bioresour Technol 2019;289:121585. https://doi.org/10.1016/j.biortech.2019.121585.

[38] Mohan A, Dutta S, Madav V. Characterization and upgradation of crude tire pyrolysis oil (CTPO) obtained from a rotating autoclave reactor. Fuel 2019;250:339–51. https://doi.org/10.1016/j.fuel.2019.03.139.

[39] Quek A, Balasubramanian R. Liquefaction of waste tires by pyrolysis for oil and chemicals - a review. J Anal Appl Pyrol 2013;101:1–16. https://doi.org/10.1016/j.jaap.2013.02.016.

[40] Lopez G, Alvarez J, Amutio M, Mkhize N.M, Danon B, van der Gryp P, et al. Waste truck-tyre processing by flash pyrolysis in a conical spouted bed reactor. Energy Convers Manag 2017;142:523–32. https://doi.org/10.1016/j.enconman.2017.03.051.

[41] Wystalska K, Malińska K, Barczak M. Poultry manure derived biochars – the impact of pyrolysis temperature on selected properties and potentials for further modifications. J Sustain Dev Energy, Water Environ Syst 2021;9:1–10. https://doi.org/10.13044/j.sdewes.d8.0337.

[42] Xu F, Wang B, Yang D, Ming X, Jiang Y, Hao J, et al. TG-FTIR and Py-GC/MS study on pyrolysis mechanism and products distribution of waste bicycle tire. Energy Convers Manag 2018;175:288–97. https://doi.org/10.1016/j.enconman.2018.09.013.

[43] Wang F, Gao N, Magdziarz A, Quan C. Co-pyrolysis of biomass and waste tires under high-pressure two-stage fixed bed reactor. Bioresour Technol 2022;344. https://doi.org/10.1016/j.biortech.2021.126306.

[44] Osorio-Vargas P, Lick I.D, Sobrevía F, Correa-Muriel D, Menares T, Manrique R, et al. Thermal behavior, reaction pathways and kinetic implications of using a Ni/SiO2 catalyst for waste tire pyrolysis. Waste Biomass Valoriz 2021;12:6465–79. https://doi.org/10.1007/s12649-021-01494-y.

[45] Fernández-Berridi M, González N, Mugica A, Bernicot C. Pyrolysis-FTIR and TGA techniques as tools in the characterization of blends of natural rubber and SBR. Thermochim Acta 2006;444:65–70. https://doi.org/10.1016/j.tca.2006.02.027.

[46] Król M, Koleżyński A, Mozgawa W. Vibrational spectra of zeolite y as a function of ion exchange. Molecules 2021;26:342. https://doi.org/10.3390/molecules26020342.

[47] Hita I, Arabiourrutia M, Olazar M, Bilbao J, Arandes J.M, Castaño S.P. Opportunities and barriers for producing high quality fuels from the pyrolysis of scrap tires. Renew Sustain Energy Rev 2016;56:745–59. https://doi.org/10.1016/j.rser.2015.11.081.

[48] Wanignon Ferdinand F, Van De Steene L, Kamenan Blaise K, Siaka T. Prediction of pyrolysis oils higher heating value with gas chromatography-mass spectrometry. Fuel 2012;96:141–5. https://doi.org/10.1016/j.fuel.2012.01.007.

[49] Muenpol S, Yuwapornpanit R, Jitkarnka S. Valuable petrochemicals, petroleum fractions, and sulfur compounds in oils derived from waste tyre pyrolysis using five commercial zeolites as catalysts: impact of zeolite properties. Clean Techn Environ Policy 2015;17:1149–59. https://doi.org/10.1007/s10098-015-0935-8.

[50] Arabiourrutia M, Lopez G, Elordi G, Olazar M, Aguado R, Bilbao J. Product distribution obtained in the pyrolysis of tyres in a conical spouted bed reactor. Chem Eng Sci 2007;62:5271–5. https://doi.org/10.1016/j.ces.2006.12.026.

[51] Campuzano F, Ordoñez J, Martínez J.D, Agudelo A.F, Sarathy S.M, Roberts W.L. Thermal decomposition characteristics of the tire pyrolysis oil derived from a twin-auger reactor: study of kinetics and evolved gases. Fuel 2023;338:127248. https://doi.org/10.1016/j.fuel.2022.127248.

[52] Jameel A.G.A, Alquaity A.B.S, Islam K.M.O, Pasha A.A, Khan S, Nemitallah M.A, et al. Pyrolysis and oxidation of waste tire oil: analysis of evolved gases. ACS Omega 2022;7:21574–82. https://doi.org/10.1021/acsomega.2c01366.

[53] Stančin H, Mikulčić H, Manić N, Stojiljković D, Vujanović M. Thermogravimetric and kinetic analysis of waste biomass and plastic mixtures. J Sustain Dev Energy, Water Environ Syst 2023;11:1110469. https://doi.org/10.13044/j.sdewes.d11.0469.

[54] Zhao S, Pu W, Varfolomeev M.A, Liu Y, Liu Z. Oxidation characteristics of heavy oil and its SARA fractions during combustion using TG-FTIR. J Pet Sci Eng 2020;192:107331. https://doi.org/10.1016/j.petrol.2020.107331.

[55] Al-Rahbi A.S, Williams P.T. Waste ashes as catalysts for the pyrolysis–catalytic steam reforming of biomass for hydrogen-rich gas production. J Mater Cycles Waste Manag 2019;21:1224–31. https://doi.org/10.1007/s10163-019-00876-8.

[56] Raza J, Khoja A.H, Naqvi S.R, Mehran M.T, Shakir S, Liaquat R, et al. Methane decomposition for hydrogen production over biomass fly ash-based CeO2 nanowires promoted cobalt catalyst. J Environ Chem Eng 2021;9:105816. https://doi.org/10.1016/j.jece.2021.105816.

[57] Mubari P.-K, Weiss E, Monthioux M, Moyano S, Bowles A, Fowler G, et al. Analysing the modifications of carbon black and other fillers after pyrolysis of model tyres. Sustain Mater Technol 2024;40:e00904.

[58] Olson D.H, Haag W.O, Lago R.M. Chemical and physical properties of the ZSM-5 substitutional series. J Catal 1980;61:390–6. https://doi.org/10.1016/0021-9517(80)90386-3.
[59] Zhou N, Dai L, Lyu Y, Wang Y, Li H, Cobb K, et al. A structured catalyst of ZSM-5/SiC foam for chemical recycling of waste plastics via catalytic pyrolysis. Chem Eng J 2022;440:135836. https://doi.org/10.1016/j.cej.2022.135836.
[60] Mukarakate C, Watson M.J, Ten Dam J, Baucherel X, Budhi S, Yung M.M, et al. Upgrading biomass pyrolysis vapors over β-zeolites: role of silica-to-alumina ratio. Green Chem 2014;16:4891–905. https://doi.org/10.1039/c4gc01425a.
[61] Artetxe M, Lopez G, Amutio M, Elordi G, Bilbao J, Olazar M. Cracking of high density polyethylene pyrolysis waxes on HZSM-5 catalysts of different acidity. Ind Eng Chem Res 2013;52:10637–45. https://doi.org/10.1021/ie4014869.
[62] Bowles A.J, Wilson A.L, Fowler G.D. Synergistic benefits of recovered carbon black demineralisation for tyre recycling. Resour Conserv Recycl 2023;198:107124. https://doi.org/10.1016/j.resconrec.2023.107124.
[63] Thonglhueng N, Sirisangsawang R, Sukpancharoen S, Phetyim N. Optimization of iodine number of carbon black obtained from waste tire pyrolysis plant via response surface methodology. Heliyon 2022;8:e11971.
[64] Zhang G, Jiang Y, Wang S, Zhang Y. Influence of a novel coupling agent on the performance of recovered carbon black filled natural rubber. Compos B Eng 2023;255:110614. https://doi.org/10.1016/j.compositesb.2023.110614.
[65] Guisnet M, Costa L, Ribeiro F.R. Prevention of zeolite deactivation by coking. J Mol Catal A Chem 2009;305:69–83. https://doi.org/10.1016/j.molcata.2008.11.012.